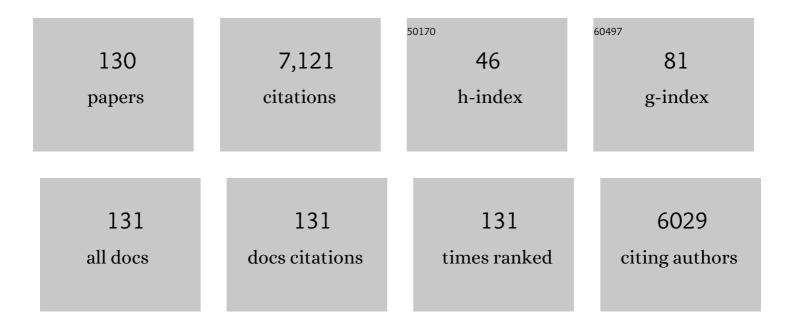
Jiang-Wen Liu

List of Publications by Year in descending order

Source: https://exaly.com/author-pdf/4642419/publications.pdf Version: 2024-02-01



IANC-WEN LUI

#	Article	IF	CITATIONS
1	New Nanoconfined Galvanic Replacement Synthesis of Hollow Sb@C Yolk–Shell Spheres Constituting a Stable Anode for High-Rate Li/Na-Ion Batteries. Nano Letters, 2017, 17, 2034-2042.	4.5	386
2	A General Metalâ€Organic Framework (MOF)â€Derived Selenidation Strategy for In Situ Carbonâ€Encapsulated Metal Selenides as Highâ€Rate Anodes for Naâ€Ion Batteries. Advanced Functional Materials, 2018, 28, 1707573.	7.8	325
3	Enhancing the Regeneration Process of Consumed NaBH ₄ for Hydrogen Storage. Advanced Energy Materials, 2017, 7, 1700299.	10.2	304
4	Mg–TM (TM: Ti, Nb, V, Co, Mo or Ni) core–shell like nanostructures: synthesis, hydrogen storage performance and catalytic mechanism. Journal of Materials Chemistry A, 2014, 2, 9645-9655.	5.2	248
5	Robust Pitaya-Structured Pyrite as High Energy Density Cathode for High-Rate Lithium Batteries. ACS Nano, 2017, 11, 9033-9040.	7.3	247
6	Remarkable enhancement in dehydrogenation of MgH2 by a nano-coating of multi-valence Ti-based catalysts. Journal of Materials Chemistry A, 2013, 1, 5603.	5.2	221
7	Mechanistic Understanding of Metal Phosphide Host for Sulfur Cathode in High-Energy-Density Lithium–Sulfur Batteries. ACS Nano, 2019, 13, 8986-8996.	7.3	215
8	Progress of hydrogen storage alloys for Ni-MH rechargeable power batteries in electric vehicles: A review. Materials Chemistry and Physics, 2017, 200, 164-178.	2.0	207
9	Magnesium-based hydrogen storage compounds: A review. Journal of Alloys and Compounds, 2020, 832, 154865.	2.8	206
10	Closing the Loop for Hydrogen Storage: Facile Regeneration of NaBH ₄ from its Hydrolytic Product. Angewandte Chemie - International Edition, 2020, 59, 8623-8629.	7.2	205
11	Hydrolysis and regeneration of sodium borohydride (NaBH 4) – A combination of hydrogen production and storage. Journal of Power Sources, 2017, 359, 400-407.	4.0	173
12	Symbiotic CeH 2.73 /CeO 2 catalyst: A novel hydrogen pump. Nano Energy, 2014, 9, 80-87.	8.2	159
13	Converting H ⁺ from coordinated water into H ^{â^'} enables super facile synthesis of LiBH ₄ . Green Chemistry, 2019, 21, 4380-4387.	4.6	149
14	Mesoporous Mo ₂ C/N-doped carbon heteronanowires as high-rate and long-life anode materials for Li-ion batteries. Journal of Materials Chemistry A, 2016, 4, 10842-10849.	5.2	143
15	A mechanical-force-driven physical vapour deposition approach to fabricating complex hydride nanostructures. Nature Communications, 2014, 5, 3519.	5.8	136
16	Metal–Organic Framework-Derived NiSb Alloy Embedded in Carbon Hollow Spheres as Superior Lithium-Ion Battery Anodes. ACS Applied Materials & Interfaces, 2017, 9, 2516-2525.	4.0	116
17	Altered desorption enthalpy of MgH2 by the reversible formation of Mg(In) solid solution. Scripta Materialia, 2011, 65, 285-287.	2.6	108
18	Air-stable hydrogen generation materials and enhanced hydrolysis performance of MgH 2 -LiNH 2 composites. Journal of Power Sources, 2017, 359, 427-434.	4.0	103

#	Article	IF	CITATIONS
19	Hydrogen generation via hydrolysis of magnesium with seawater using Mo, MoO ₂ , MoO ₃ and MoS ₂ as catalysts. Journal of Materials Chemistry A, 2017, 5, 8566-8575.	5.2	103
20	FeP@C Nanotube Arrays Grown on Carbon Fabric as a Low Potential and Freestanding Anode for Highâ€Performance Liâ€Ion Batteries. Small, 2018, 14, e1800793.	5.2	94
21	Express penetration of hydrogen on Mg(10ĺž13) along the close-packed-planes. Scientific Reports, 2015, 5, 10776.	1.6	89
22	A long-life nano-silicon anode for lithium ion batteries: supporting of graphene nanosheets exfoliated from expanded graphite by plasma-assisted milling. Electrochimica Acta, 2016, 187, 1-10.	2.6	89
23	Unraveling the Catalytic Activity of Fe–Based Compounds toward Li ₂ S <i>_x</i> in Li–S Chemical System from <i>d</i> – <i>p</i> Bands. Advanced Energy Materials, 2021, 11, 2100673.	10.2	89
24	A new method for few-layer graphene preparation via plasma-assisted ball milling. Journal of Alloys and Compounds, 2017, 728, 578-584.	2.8	86
25	Sn–C and Se–C Co-Bonding SnSe/Few-Layered Graphene Micro–Nano Structure: Route to a Densely Compacted and Durable Anode for Lithium/Sodium-Ion Batteries. ACS Applied Materials & Interfaces, 2019, 11, 36685-36696.	4.0	83
26	Constructing Liâ€Rich Artificial SEI Layer in Alloy–Polymer Composite Electrolyte to Achieve High Ionic Conductivity for Allâ€Solidâ€State Lithium Metal Batteries. Advanced Materials, 2021, 33, e2004711.	11.1	82
27	Advanced high-pressure metal hydride fabricated via Ti–Cr–Mn alloys for hybrid tank. International Journal of Hydrogen Energy, 2015, 40, 2717-2728.	3.8	81
28	Selfâ€Supported CoP Nanorod Arrays Grafted on Stainless Steel as an Advanced Integrated Anode for Stable and Longâ€Life Lithiumâ€lon Batteries. Chemistry - A European Journal, 2017, 23, 5198-5204.	1.7	75
29	Facile synthesis of Ge@FLG composites by plasma assisted ball milling for lithium ion battery anodes. Journal of Materials Chemistry A, 2014, 2, 11280-11285.	5.2	74
30	A highly stable (SnO x -Sn)@few layered graphene composite anode of sodium-ion batteries synthesized by oxygen plasma assisted milling. Journal of Power Sources, 2017, 350, 1-8.	4.0	74
31	Development of ZrFeV alloys for hybrid hydrogen storage system. International Journal of Hydrogen Energy, 2016, 41, 11242-11253.	3.8	71
32	Facilitating de/hydrogenation by long-period stacking ordered structure in Mg based alloys. International Journal of Hydrogen Energy, 2013, 38, 10438-10445.	3.8	70
33	Sandwiched MoS2/polyaniline nanosheets array vertically aligned on reduced graphene oxide for high performance supercapacitors. Electrochimica Acta, 2018, 270, 387-394.	2.6	64
34	Composition design of Ti–Cr–Mn–Fe alloys for hybrid high-pressure metal hydride tanks. Journal of Alloys and Compounds, 2015, 639, 452-457.	2.8	63
35	A spherical Sn–Fe ₃ O ₄ @graphite composite as a long-life and high-rate-capability anode for lithium ion batteries. Journal of Materials Chemistry A, 2016, 4, 10321-10328.	5.2	63
36	Lithium Difluorophosphate As a Promising Electrolyte Lithium Additive for High-Voltage Lithium-Ion Batteries. ACS Applied Energy Materials, 2018, 1, 2647-2656.	2.5	60

#	Article	IF	CITATIONS
37	Hierarchical nanoflowers assembled from MoS 2 /polyaniline sandwiched nanosheets for high-performance supercapacitors. Electrochimica Acta, 2017, 243, 98-104.	2.6	56
38	Sn buffered by shape memory effect of NiTi alloys as high-performance anodes for lithium ion batteries. Acta Materialia, 2012, 60, 4695-4703.	3.8	53
39	Progress on Sn-based thin-film anode materials for lithium-ion batteries. Science Bulletin, 2012, 57, 4119-4130.	1.7	53
40	Fully Reversible De/hydriding of Mg Base Solid Solutions with Reduced Reaction Enthalpy and Enhanced Kinetics. Journal of Physical Chemistry C, 2014, 118, 12087-12096.	1.5	53
41	Co-Substitution Enhances the Rate Capability and Stabilizes the Cyclic Performance of O3-Type Cathode NaNi _{0.45–<i>x</i>} Mn _{0.25} Ti _{0.3} Co _{<i>x</i>} O ₂ for Sodium-Ion Storage at High Voltage. ACS Applied Materials & Interfaces, 2019, 11, 7906-7913.	4.0	53
42	Towards easy reversible dehydrogenation of LiBH 4 by catalyzing hierarchic nanostructured CoB. Nano Energy, 2014, 10, 235-244.	8.2	52
43	Hydrogen generation from sodium borohydride hydrolysis accelerated by zinc chloride without catalyst: A kinetic study. Journal of Alloys and Compounds, 2017, 717, 48-54.	2.8	51
44	Structural characteristics and hydrogen storage properties of Sm2Co7. Journal of Alloys and Compounds, 2014, 608, 14-18.	2.8	48
45	Phase transition and hydrogen storage properties of Mg–Ga alloy. Journal of Alloys and Compounds, 2015, 642, 180-184.	2.8	47
46	Comparative investigation on the hydrogenation/dehydrogenation characteristics and hydrogen storage properties of Mg3Ag and Mg3Y. International Journal of Hydrogen Energy, 2014, 39, 13616-13621.	3.8	46
47	Deformable fibrous carbon supported ultrafine nano-SnO ₂ as a high volumetric capacity and cyclic durable anode for Li storage. Journal of Materials Chemistry A, 2015, 3, 15097-15107.	5.2	46
48	Enhancing the performance of Sn–C nanocomposite as lithium ion anode by discharge plasma assisted milling. Journal of Materials Chemistry, 2012, 22, 8022.	6.7	44
49	Growth mechanism of black phosphorus synthesized by different ball milling techniques. Journal of Alloys and Compounds, 2019, 784, 339-346.	2.8	44
50	3,3′-(Ethylenedioxy)dipropiononitrile as an Electrolyte Additive for 4.5 V LiNi _{1/3} Co _{1/3} Mn _{1/3} O ₂ /Graphite Cells. ACS Applied Materials & Interfaces, 2017, 9, 9630-9639.	4.0	43
51	Origin of Capacity Increasing in a Longâ€Life Ternary Sn–Fe ₃ O ₄ @Graphite Anode for Liâ€Ion Batteries. Advanced Materials Interfaces, 2017, 4, 1700113.	1.9	43
52	Facile synthesis of self-supported Mn ₃ O ₄ @C nanotube arrays constituting an ultrastable and high-rate anode for flexible Li-ion batteries. Journal of Materials Chemistry A, 2017, 5, 8555-8565.	5.2	41
53	Destabilizing the dehydriding thermodynamics of MgH2 by reversible intermetallics formation in Mgâ^'Agâ^'Zn ternary alloys. Journal of Power Sources, 2018, 396, 796-802.	4.0	39
54	Realizing facile regeneration of spent NaBH ₄ with Mg–Al alloy. Journal of Materials Chemistry A, 2019, 7, 10723-10728.	5.2	39

#	Article	IF	CITATIONS
55	Closing the Loop for Hydrogen Storage: Facile Regeneration of NaBH ₄ from its Hydrolytic Product. Angewandte Chemie, 2020, 132, 8701-8707.	1.6	39
56	An amorphous wrapped nanorod LiV3O8 electrode with enhanced performance for lithium ion batteries. RSC Advances, 2012, 2, 7273.	1.7	37
57	Nanoconfined Oxidation Synthesis of Nâ€Doped Carbon Hollow Spheres and MnO ₂ Encapsulated Sulfur Cathode for Superior Li Batteries. Chemistry - A European Journal, 2018, 24, 4573-4582.	1.7	34
58	Engineering layer structure of MoS2/polyaniline/graphene nanocomposites to achieve fast and reversible lithium storage for high energy density aqueous lithium-ion capacitors. Journal of Power Sources, 2020, 450, 227680.	4.0	33
59	Overview of hydrogen compression materials based on a three-stage metal hydride hydrogen compressor. Journal of Alloys and Compounds, 2022, 895, 162465.	2.8	33
60	Silicon/Wolfram Carbide@Graphene composite: enhancing conductivity and structure stability in amorphous-silicon for high lithium storage performance. Electrochimica Acta, 2016, 191, 462-472.	2.6	32
61	Oxygen-Incorporated and Polyaniline-Intercalated 1T/2H Hybrid MoS2 Nanosheets Arrayed on Reduced Graphene Oxide for High-Performance Supercapacitors. Journal of Physical Chemistry C, 2018, 122, 8128-8136.	1.5	32
62	Nano-spatially confined and interface-controlled lithiation–delithiation in an <i>in situ</i> formed (SnS–SnS ₂ –S)/FLG composite: a route to an ultrafast and cycle-stable anode for lithium-ion batteries. Journal of Materials Chemistry A, 2019, 7, 15320-15332.	5.2	32
63	Chemical bonding black phosphorus with TiO2 and carbon toward high-performance lithium storage. Journal of Power Sources, 2020, 449, 227549.	4.0	32
64	Exfoliation of MoS ₂ and h-BN nanosheets by hydrolysis of LiBH ₄ . Nanotechnology, 2017, 28, 115604.	1.3	30
65	Reversible hydrogen storage in yttrium aluminum hydride. Journal of Materials Chemistry A, 2017, 5, 6042-6046.	5.2	29
66	Citraconic anhydride as an electrolyte additive to improve the high temperature performance of LiNiO·6CoO·2MnO·2O2/graphite pouch batteries. Journal of Alloys and Compounds, 2019, 805, 757-766.	2.8	29
67	A phosphorus and carbon composite containing nanocrystalline Sb as a stable and high-capacity anode for sodium ion batteries. Journal of Materials Chemistry A, 2020, 8, 443-452.	5.2	29
68	Controllable Hydrolysis Performance of MgLi Alloys and Their Hydrides. ChemPhysChem, 2019, 20, 1316-1324.	1.0	27
69	Adding Metal Carbides to Suppress the Crystalline Li15Si4 Formation: A Route toward Cycling Durable Si-Based Anodes for Lithium-Ion Batteries. ACS Applied Materials & Interfaces, 2019, 11, 38727-38736.	4.0	26
70	Reversible De/hydriding Reactions between Two New Mg–In–Ni Compounds with Improved Thermodynamics and Kinetics. Journal of Physical Chemistry C, 2015, 119, 26858-26865.	1.5	25
71	Dualâ€Carbon onfined SnS Nanostructure with High Capacity and Long Cycle Life for Lithiumâ€ion Batteries. Energy and Environmental Materials, 2021, 4, 562-568.	7.3	24
72	Microsized Sn supported by NiTi alloy as a high-performance film anode for Li-ion batteries. Journal of Materials Chemistry, 2012, 22, 9539.	6.7	23

#	Article	IF	CITATIONS
73	Improving hydrogen storage properties of MgH2 by addition ofÂalkali hydroxides. International Journal of Hydrogen Energy, 2013, 38, 10932-10938.	3.8	23
74	Achieving high equilibrium pressure and low hysteresis of Zr–Fe based hydrogen storage alloy by Cr/V substitution. Journal of Alloys and Compounds, 2019, 806, 1436-1444.	2.8	23
75	High-pressure hydrogen storage performances of ZrFe2 based alloys with Mn, Ti, and V addition. International Journal of Hydrogen Energy, 2020, 45, 9836-9844.	3.8	23
76	The milled LiBH 4 / h- BN composites exhibiting unexpected hydrogen storage kinetics and reversibility. International Journal of Hydrogen Energy, 2017, 42, 15790-15798.	3.8	21
77	Microsized SnS/Fewâ€Layer Graphene Composite with Interconnected Nanosized Building Blocks for Superior Volumetric Lithium and Sodium Storage. Energy and Environmental Materials, 2021, 4, 229-238.	7.3	21
78	Hydrogen-Induced Reversible Phase Transformations and Hydrogen Storage Properties of Mg–Ag–Al Ternary Alloys. Journal of Physical Chemistry C, 2016, 120, 27117-27127.	1.5	19
79	Reversible hydriding in YFe Al (x= 0.3, 0.5, 0.7) intermetallic compounds. Journal of Alloys and Compounds, 2016, 689, 843-848.	2.8	19
80	Enhanced cyclic stability of SnS microplates with conformal carbon coating derived from ethanol vapor deposition for sodium-ion batteries. Applied Surface Science, 2018, 436, 912-918.	3.1	19
81	Direct Detection and Visualization of the H ⁺ Reaction Process in a VO ₂ Cathode for Aqueous Zinc-Ion Batteries. Journal of Physical Chemistry Letters, 2021, 12, 7076-7084.	2.1	19
82	Improved coulombic efficiency and cycleability of SnO ₂ –Cu–graphite composite anode with dual scale embedding structure. RSC Advances, 2016, 6, 13384-13391.	1.7	17
83	Efficient Synthesis of Sodium Borohydride: Balancing Reducing Agents with Intrinsic Hydrogen Source in Hydrated Borax. ACS Sustainable Chemistry and Engineering, 2020, 8, 13449-13458.	3.2	17
84	Ti-Cr-Mn-Fe-based alloys optimized by orthogonal experiment for 85ÂMPa hydrogen compression materials. Journal of Alloys and Compounds, 2022, 891, 161791.	2.8	17
85	Reducing the electrochemical capacity decay of milled Mg–Ni alloys: The role of stabilizing amorphous phase by Ti-substitution. Journal of Power Sources, 2019, 438, 226984.	4.0	16
86	Regulation of high-efficient regeneration of sodium borohydride by magnesium-aluminum alloy. International Journal of Hydrogen Energy, 2019, 44, 29108-29115.	3.8	16
87	Metallic Ni nanocatalyst in situ formed from LaNi5H5 toward efficient CO2 methanation. International Journal of Hydrogen Energy, 2019, 44, 29068-29074.	3.8	16
88	Reaction Route Optimized LiBH ₄ for High Reversible Capacity Hydrogen Storage by Tunable Surface-Modified AlN. ACS Applied Energy Materials, 2020, 3, 11964-11973.	2.5	16
89	Tuning hydrogen storage thermodynamic properties of ZrFe2 by partial substitution with rare earth element Y. International Journal of Hydrogen Energy, 2021, 46, 18445-18452.	3.8	16
90	Effective synthesis of magnesium borohydride via B-O to B-H bond conversion. Chemical Engineering Journal, 2022, 432, 134322.	6.6	16

#	Article	IF	CITATIONS
91	H ₂ Plasma Reducing Ni Nanoparticles for Superior Catalysis on Hydrogen Sorption of MgH ₂ . ACS Applied Energy Materials, 2022, 5, 4976-4984.	2.5	16
92	Phase transformation and hydrogen storage properties of LaY2Ni10.5 superlattice alloy with single Gd2Co7-type or Ce2Ni7-type structure. Journal of Alloys and Compounds, 2021, 868, 159254.	2.8	15
93	Reversible hydrogen storage and phase transformation with altered desorption pressure in Mg90In5Cd5 ternary alloy. Journal of Alloys and Compounds, 2015, 645, S103-S106.	2.8	14
94	Hydrogen generation properties and the hydrolysis mechanism of Zr(BH ₄) ₄ ·8NH ₃ . Journal of Materials Chemistry A, 2017, 5, 16630-16635.	5.2	14
95	Achieving High Dehydrogenation Kinetics and Reversibility of LiBH ₄ by Adding Nanoporous h-BN to Destabilize LiH. Journal of Physical Chemistry C, 2018, 122, 23336-23344.	1.5	14
96	Exploration of Ti substitution in AB2-type Y Zr Fe based hydrogen storage alloys. International Journal of Hydrogen Energy, 2019, 44, 29116-29122.	3.8	14
97	High speed abrasive electrical discharge machining of particulate reinforced metal matrix composites. International Journal of Precision Engineering and Manufacturing, 2015, 16, 1399-1404.	1.1	13
98	Low temperature de/hydrogenation in the partially crystallized Mg60Ce10Ni20Cu10 metallic glasses induced by milling with process control agents. Journal of Alloys and Compounds, 2019, 792, 835-843.	2.8	13
99	Enhanced hydrogen generation performance of CaMg ₂ -based materials by ball milling. Inorganic Chemistry Frontiers, 2020, 7, 918-929.	3.0	13
100	Flowerlike Ti-Doped MoO ₃ Conductive Anode Fabricated by a Novel NiTi Dealloying Method: Greatly Enhanced Reversibility of the Conversion and Intercalation Reaction. ACS Applied Materials & Interfaces, 2020, 12, 8240-8248.	4.0	13
101	In-situ introducing TiP2 nanocrystals in black phosphorus anode to promote high rate-capacity synergy. Journal of Power Sources, 2021, 499, 229979.	4.0	13
102	The Electrolyte Additive Effects on Commercialized Ni-Rich LiNi _{<i>x</i>} Co <i>_y</i> Mn <i>z</i> O ₂ (<i>x</i> + <i>y</i> + <i>z</i>) Tj E 2292-2299.	TQ <u>q</u> 0 0 0	rgBT /Overloc
103	Growth twinning behavior of cast Mg–Zn–Cu–Zr alloys. Transactions of Nonferrous Metals Society of China, 2014, 24, 316-320.	1.7	11
104	Achieving superior de-/hydrogenation properties of C15 Laves phase Y-Fe-Al alloys by A-side substitution. Journal of Alloys and Compounds, 2019, 787, 158-164.	2.8	11
105	High Damping of Lightweight TiNi-Ti2Ni Shape Memory Composites for Wide Temperature Range Usage. Journal of Materials Engineering and Performance, 2017, 26, 4970-4976.	1.2	10
106	Improving dehydrogenation properties of Mg/Nb composite films via tuning Nb distributions. Rare Metals, 2017, 36, 574-580.	3.6	10
107	Exploring the Hydrogen-Induced Amorphization and Hydrogen Storage Reversibility of Y(Sc)0.95Ni2 Laves Phase Compounds. Materials, 2021, 14, 276.	1.3	10
108	An Al–Li alloy/water system for superior and low-temperature hydrogen production. Inorganic Chemistry Frontiers, 2021, 8, 3473-3481.	3.0	10

Jiang-Wen Liu

#	Article	IF	CITATIONS
109	Improvement in the Electrochemical Lithium Storage Performance of MgH2. Inorganics, 2018, 6, 2.	1.2	9
110	Hydrogenation and crystallization of amorphous phase: A new mechanism for the electrochemical capacity and its decay in milled Mg Ni alloys. Electrochimica Acta, 2019, 305, 145-154.	2.6	9
111	Increasing de-/hydriding capacity and equilibrium pressure by designing non-stoichiometry in Al-substituted YFe2 compounds. Journal of Alloys and Compounds, 2017, 704, 491-498.	2.8	8
112	Microstructural evolution and hydrogen storage properties of Mg1-xNbx(x=0.17~0.76) alloy films via Co-Sputtering. International Journal of Hydrogen Energy, 2019, 44, 29100-29107.	3.8	8
113	Direct Microstructural Evidence on the Catalyzing Mechanism for De/hydrogenation of Mg by Multi-valence NbOx. Journal of Physical Chemistry C, 2020, 124, 6571-6579.	1.5	7
114	Breaking the Passivation: Sodium Borohydride Synthesis by Reacting Hydrated Borax with Aluminum. Chemistry - A European Journal, 2021, 27, 9087-9093.	1.7	6
115	Achieving a novel solvent-free regeneration of LiBH4 combining hydrogen storage and production in a closed material cycle. Journal of Magnesium and Alloys, 2023, 11, 1697-1708.	5.5	6
116	Comparative study of Ga and Al alloying with ZrFe2 for high-pressure hydrogen storage. International Journal of Hydrogen Energy, 2022, 47, 13409-13417.	3.8	6
117	Promoting the cycling stability of amorphous MgNi-based alloy electrodes by mitigating hydrogen-induced crystallization. International Journal of Hydrogen Energy, 2021, 46, 6701-6708.	3.8	5
118	Hydrogen Transportation Behaviour of V–Ni Solid Solution: A First-Principles Investigation. Materials, 2021, 14, 2603.	1.3	5
119	Synthesis of NaBH ₄ as a hydrogen carrier from hydrated borax using a Mg–Al alloy. Inorganic Chemistry Frontiers, 2022, 9, 370-378.	3.0	5
120	Using tetramethylammonium hydroxide electrolyte to inhibit corrosion of Mg-based amorphous alloy anodes: A route for promotion energy density of Ni-MH battery. Journal of Alloys and Compounds, 2022, 907, 164293.	2.8	5
121	Effect of scandium and zirconium alloying on microstructure and gaseous hydrogen storage properties of YFe3. Journal of Rare Earths, 2022, 40, 467-472.	2.5	4
122	N-Doped Carbon Coated SnS/rGO Composite with Superior Cyclic Stability as Anode for Lithium-Ion Batteries. Industrial & Engineering Chemistry Research, 2022, 61, 4339-4347.	1.8	4
123	Improving hydrogen-induced crystallization and electrochemical hydrogen storage properties of MgNi amorphous alloy with CoB addition. Journal of Non-Crystalline Solids, 2022, 588, 121646.	1.5	4
124	Invariant Deformation Element Model Interpretation to the Crystallography of Diffusional Body-Centered-Cube to Face-Centered-Cube Phase Transformations. Metallurgical and Materials Transactions A: Physical Metallurgy and Materials Science, 2012, 43, 3636-3641.	1.1	3
125	Na-Ion Batteries: A General Metal-Organic Framework (MOF)-Derived Selenidation Strategy for In Situ Carbon-Encapsulated Metal Selenides as High-Rate Anodes for Na-Ion Batteries (Adv. Funct. Mater.) Tj ETQq1 1 C	.78. 8 314 r	g B T /Overl <mark>oc</mark> l
126	Li–S Batteries: Unraveling the Catalytic Activity of Fe–Based Compounds toward Li ₂ S <i>_x</i> in Li–S Chemical System from <i>d</i> – <i>p</i> Bands (Adv.) Tj ETQe	0 1@@ rgB	T /Øverlock 1

#	Article	IF	CITATIONS
127	Analysis of port and inland transport mode selection. , 2014, , .		1
128	Nanoconfined Oxidation Synthesis of Nâ€Doped Carbon Hollow Spheres and MnO 2 Encapsulated Sulfur Cathode for Superior Liâ€S Batteries. Chemistry - A European Journal, 2018, 24, 4472-4472.	1.7	1
129	Li-Ion Batteries: FeP@C Nanotube Arrays Grown on Carbon Fabric as a Low Potential and Freestanding Anode for High-Performance Li-Ion Batteries (Small 30/2018). Small, 2018, 14, 1870138.	5.2	1
130	Box office forecasting for a cinema with movie and cinema attributes. , 2018, , .		1